Helically Fixed Chiral Bilirubins and Biliverdins: A New Insight into the Conformational, Associative and Dynamic Features of Linear Tetrapyrrols

Daniel Krois and Harald Lehner*
Institut für Organische Chemie der Universität Wien, Währingerstraße 38, A-1090 Wien, Österreich

The 2,18-bridged biliverdins **1**, **2** and **5** and bilirubins **3**, **4** and **6** each forced into a helical conformation have been prepared and investigated by UV–VIS spectroscopy, ^{1}H NMR spectroscopy techniques and vapour pressure osmometry. Barriers to interconversion of the tetrapyrrole moieties of *M* and *P* chirality were accomplished by kinetic measurements of partially resolved materials using CD spectroscopy. These results were compared with those obtained for non-bridged analogues reported here and in the literature. Based on the above, the structural and environmental factors controlling the dynamic, associative and conformational behaviour of biliverdins and bilirubins have been established. In this connection the complete conformational and associative pattern of bilirubin-IXα-dimethyl ester (**10**) is presented.

The most prominent members of linear tetrapyrroles are found among biladienes-ac (bilirubins) and bilatrienes-abc (biliverdins). Bilatrienes provide the cofactor responsible for photomorphogenesis in higher plants and even occur in the photosynthetic apparatus of procaryotes.[1] In animals biliverdin-IXα (**7**) and bilirubin-IXα (**9**) appear as metabolites and accumulation of the latter causes severe intoxication.[2] These compounds are distinguished by their pronounced tendency to form inter- and/or intra-molecular hydrogen bonds.[3] They have this property in common with peptides owing to the similarity of donor and acceptor sites provided by the heterocyclic entities and the amide groups, respectively. Owing to their conformational mobility any operation, structural or environmental, which modifies strength and/or orientation of hydrogen bonding forces may simultaneously change the three dimensional arrangement. It is this property which often seriously impedes their investigation or gives rise to an uncertainty in the interpretation of results. To overcome these difficulties the synthesis of conformationally restricted analogues of biliverdins and bilirubins has become a challenging target in recent years. In the meantime numerous compounds adopting various defined stretched molecular arrangements have been synthesised.[4–7] However, examples for restricted helicoidal conformers[7–9] are rare, especially in the bilirubin family where only one example is known.[9] Recently we reported[8] on the synthesis of the helically fixed biliverdin **2** by oxidative ring closure of biliverdin-IIIα resulting in a C_4 link between rings A and D. This approach to freeze geometry comprises one of the two rare examples (see also ref. 7) which avoids substitution at nitrogen so that all hydrogen bonding sites are preserved. This condition is prerequisite for a reliable comparison with naturally occurring non-bridged analogues. The convenient access of **2** prompted us to extend our conformational studies to the bilirubin family. This seemed important since for biladienes-ac a comprehensive correlation of experimental data with the diverse conformational and associative patterns is lacking so far[3] although considerable effort has been devoted on that subject.[10–16]

This report deals with the synthesis and stereochemical assignment of ('all *Z*, all *syn*') bilirubins and biliverdins, their dynamic, associative and spectroscopic properties and the implications for the conformational behaviour of open chain analogues.

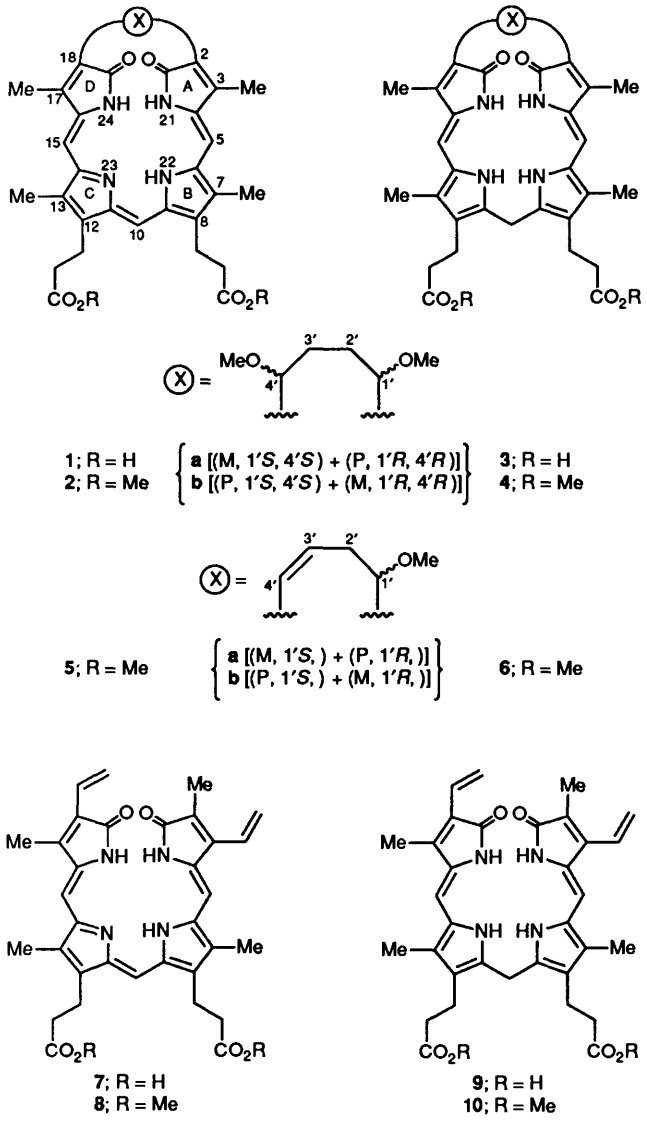

Results and Discussion

Syntheses and Stereochemical Assignments.—For the syntheses of the macrocycles **3**–**6** given in this account the biliverdins **1** and **2** served as precursors.[8] If compound **2** is treated for 1 min (0 °C) with concentrated sulfuric acid and reaction then quenched with methanol the unsaturated verdin **5** is obtained (yield 52%) by formal elimination of one equivalent

Table 1 Equilibrium distributions (%) of **a** and **b** species of 2,18-bridged biliverdins and bilirubins[a]

	2[b]		3		4		5		6	
Methanol	80	20	66	34	64	36	80	20	70	30
Ethanol	74	26					75	25		
Chloroform	72	28	64	36	50	50	80	20		
DMSO	71	29			36	64				
Pyridine	60	40	30	70	33	67	68	32	60	40
Benzene	30	70			20	80	55	45		

[a] By integrating the corresponding ^{1}H NMR absorptions due to 1'-H (and 4'-H), and/or 1'-OMe (and 4'-OMe) at 293 K; error ±2%; distributions not listed have not been determined. [b] With exception of pyridine, values were taken from ref. 8.

methanol. Higher temperatures or longer reaction times favour the formation of polymers. Using deuteriated reagents deuterium is found in the methoxy group of the product **5** but in no other position of the bridge. This suggests that on dissolution of compound **2** in sulfuric acid a carbocation **I** is generated to which

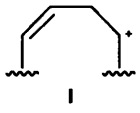

I

one methoxy group is re-added on subsequent treatment with methanol. A corresponding diene formed by elimination of two equivalents of methanol could not be detected. Also, concluded from the deuteriation experiment, such an intermediate diene, if formed at all, is consumed by side reactions (*e.g.* cationic polymerisation) faster than its reprotonation to **I** takes place. Sodium borohydride reductions of the biliverdins **1**, **2** and **5** in methanol proceeded smoothly to give the corresponding bilirubins **3**, **4** and **6**, respectively, in high yields (> 90%).

For each of the bridged tetrapyrroles **1**–**6** two diastereoisomeric pairs of enantiomers, **a** and **b** exist, carrying at least one chirality centre of configuration *R* or *S*. If two centres occur (**1**–**4**) configurations are homochiral, (1'*R*,4'*R*) or (1'*S*,4'*S*), as follows from the C_2-symmetry displayed in the ^{1}H and ^{13}C NMR spectra. The tetrapyrrole moiety provides an additional chirality element being of *M* or *P* helicity. Thermally promoted $M \rightleftharpoons P$ interconversion proceeds through equilibria, shown in eqns. (1) and (2), resulting in the mutual conversion of diastereoisomers **a** and **b**. (For detailed considerations on that topic see refs. 8 and 17).

$$[M,1'R,(4'R)]\text{-}\mathbf{b} \overset{K}{\rightleftharpoons} [P,1'R,(4'R)]\text{-}\mathbf{a} \quad (1)$$

$$[P,1'S,(4'S)]\text{-}\mathbf{b} \overset{K}{\rightleftharpoons} (M,1'S,(4'S)]\text{-}\mathbf{a} \quad (2)$$

The (4*Z*,15*Z*,5 *syn*,14 *syn*) geometry of all new compounds was established by NOE experiments (3-Me ↔ 5-H, 5-H ↔ 7-Me, 13-Me ↔ 15-H, 15-H ↔ 17-Me). Hence, considering the restrictions imposed on the tetrapyrrole backbones by the links between rings A and D, the stereochemical relations between rings B and C necessarily follow to be (9 *syn*,10 *syn*) for the bilirubins **3**, **4** and **6** and (10*Z*,9 *syn*) for the verdins **1**, **2** and **5**.

The coupling constants ($J_{3'4'}$ 11 Hz) between the two vinylic protons in the bridge of the diastereoisomers of **5** and **6** are indicative of the *Z* configuration of the respective $\Delta_{3'4'}$ double bond. The stereochemical assignments for **a** and **b** species of compounds **3**, **4**, **5** and **6** were assessed by NOE experiments following the approach reported for the precursor **2**[8] by considering the different spatial relationships between 3-Me(17-Me), 1'-H(4'-H) and 1'-OMe(4'-OMe). The proportions of diastereoisomers vary with the nature of the solvent (Table 1) and were evaluated as reported for **2**[8] by ^{1}H NMR spectroscopy, integrating the well resolved proton signals 1'-H and/or 1'-OMe. For **2**, **5** and **6** chromatographic separation into **a** and **b** species succeeded at ambient (**5a**/**5b**) and moderately low temperatures (**2a**/**2b** and **6a**/**6b**) respectively, but this method failed if applied to the more rapidly interconverting diastereoisomers of the bilirubins **3** and **4** (see below).

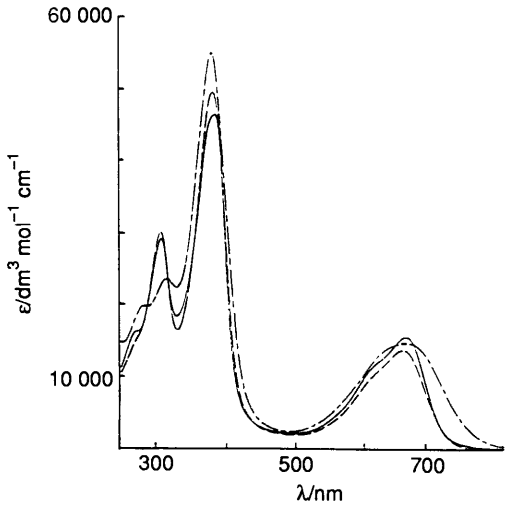

Fig. 1 UV–VIS spectra of the biliverdins **2** (——), **5** (– – –), and **8** (— · — · —) for *ca.* 3 × 10^{-5} mol dm^{-3} solutions in chloroform at 293 K

The sensitivity of UV–VIS spectra of bile pigments in general towards even subtle conformational changes allows the following conclusions to be made: (i) the geometry of the bilatriene backbone of related **a** and **b** species of compounds **2**, **5** and **6** must be very similar; (ii) the helix geometry of the verdin **2** and the rubin **4**, respectively, is not affected by introduction of the double bond in the bridge as present in **5** and **6**. This follows from the great similarity in UV–VIS spectra of the corresponding pairs considered (Table 2 and Fig. 1).

Bridged vs. *Non-Bridged Members. Conformation and Aggregation in Solution.*—Open chain, non-restricted (4*Z*,10*Z*,15*Z*) bilatrienes-abc like biliverdin-IXα-dimethyl ester (**8**) preferentially adopt a helical (5 *syn*,9 *syn*,14 *syn*) conformation in solution[3,18,19] akin to that of the restricted macrocycles **2** and **5**. Therefore, also UV–VIS spectra conform with each other (Fig. 1). Apparently, the strength of the hydrogen bonding network between donor and acceptor sites at the nitrogens is sufficiently strong to stabilise the bilatriene helix and does not require additional geometric constraints. This conformation withstands most internal and external influences. Aggregation of bilatrienes-abc in solution is not observed even in non-hydrogen bonding solvents at large concentrations (Fig. 2 and refs. 15, 18, 19).

An analogous spectral comparison drawn between members of the bilirubin family turns out to be more complex but affords valuable new information. The spectra of the bilirubins **3**, **4**, **6**, **9** and **10** comprise each an envelope of two bands centred at λ *ca.* 390 nm and λ *ca.* 450 nm, respectively, arising from exciton coupling[3,20,21] of the two non-conjugated pyrromethenone halves. Owing to this geometry dependent coupling the helicoidal conformation as relevant for the bridged compounds **3**, **4** and **6** is distinguished by the predominance of the short wavelength band around λ 390 nm. This phenotype is essentially preserved irrespective of the solvent, concentration and the nature of the propionic side chains present (Table 2 and

Table 2 UV–VIS spectra [ε_{max}/dm^3 mol^{-1} cm^{-1} (λ_{max}/nm)] of 2,18-bridged biliverdins and bilirubins[a]

	3	4	5[b]	6
Methanol	s19 500 (430) 55 200 (392)	s21 400 (427) 62 200 (387)	14 300 (657)[c] 49 000 (378) 32 600 (307)	s21 800 (429)[d] 54 700 (387)
Pyridine	s20 900 (423) 49 000 (387)	s21 600 (421) 51 000 (385)	14 500 (662) 43 900 (387) 27 700 (313)	s21 500 (425) 50 500 (388)
THF	s21 000 (412) 42 100 (378)	s25 100 (411) 56 100 (377)	14 900 (655) 46 700 (381) 29 300 (309)	s21 600 (415) 43 300 (381)
Chloroform	s24 000 (428) 44 000 (392)	s18 000 (424) 42 400 (380)	13 800 (655) 49 600 (381) 30 200 (308)	s16 000 (435) 41 300 (384)
Benzene	*e*	s17 700 (425) 45 500 (377)	16 000 (653) 49 300 (383) 30 900 (310)	s16 200 (435) 41 700 (385)

[a] *ca.* 3 × 10^{-5} mol dm^{-3} solutions, equilibrated at 293 K; spectra did not change over the concentration range 5 × 10^{-4}–1 × 10^{-6} mol dm^{-3}; for UV–VIS spectra of **2** and **2**·H$^+$ see refs. 8, 32, 36; s, shoulder; the band at λ *ca.* 310 nm is characteristically pronounced for cyclic biliverdins and is also observed for the precursors **1** and **2**. [b] Data of **5**·H$^+$ for solutions in 0.25 mol dm^{-3} methanolic H_2SO_4: 15 300 (746), 67 000 (388), 31 400 (315). [c] Data for individual species at 291 K: **5a** 14 400 (657), 48 100 (377), 31 300 (306); **5b** 14 500 (658), 49 600 (376), 31 600 (306). [d] Data for individual species at 283 K for solutions in methanol containing 1% v/v pyridine: **6a** s21 200 (430), 55 300 (387); **6b** s22 500 (425), 53 000 (385). [e] Not determined due to the low solubility.

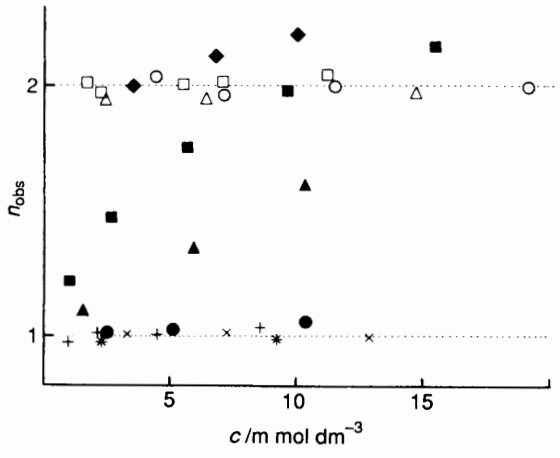

Fig. 2 Degree of association as observed by VPO (n_{obs}) *vs.* concentration for bilirubins and biliverdins; **4** (■, benzene; ▲, chloroform; ●, THF), **6** (◆, benzene), **10** (□, benzene; △, chloroform; ○, THF), **2** (+, benzene; ×, THF) and **5** (✱, chloroform)

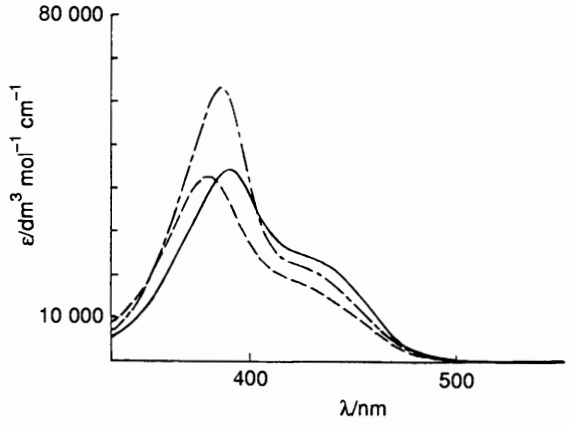

Fig. 3 UV–VIS spectra of the bilirubin **3** in chloroform (——) and the corresponding ester **4** in chloroform (– – – –) and methanol (— · — · —) for *ca.* 3 × 10^{-5} mol dm^{-3} solutions at 293 K

Fig. 3). Nevertheless, even these restricted compounds show solvent dependent UV–VIS spectra probably due to differences in helix geometries but variations in intensity of the two bands always take place in the same direction. This uniformity of the phenotype of 2,18-bridged bilirubins is in striking contrast to the great many UV–VIS spectra reported for non-bridged members. Only the spectrum of the diacid bilirubin-IXα (**9**) is essentially independent of conditions.[3,15,21] Its long and short wavelength transitions are of comparable intensity reflecting the ridge-tile like geometry.[3,21,22] The phenotype of the UV–VIS spectra of the corresponding diester **10** for solutions in methyltetrahydrofuran (MTHF), chloroform and toluene is quite different if concentrations are in the usual range (10^{-4}–10^{-5} mol dm^{-3}) (Fig. 4) and is reminiscent of that observed for the obligate helical analogues **4** and **6** (Fig. 3 and Table 2). If the concentration is lowered successively the long wavelength band increases in intensity on account of the 390 nm band until similar intensities—characteristic for the ridge-tile like conformation—are observed (Fig. 4).* The occasional concentration dependence of the ester **10** and other biladienes-ac (investigated only qualitatively up to now)†[,11,15,23] has been connected with the occurrence of dimeric aggregates.[15] However, aggregation alone cannot be responsible for these phenomena unless a synchronous conformational change takes place. In fact an eventual spectral similarity of the ester **10** with the bridged compounds **3**, **4** and **6** strongly suggests that the conformation of dimeric **10** is helical, too. This geometry has first been proposed by Manitto *et al.*[13] but doubts[10] (see also ref. 3, p. 324) have been raised. Clearly, in view of the sterically most favourable ridge-tile like conformation of biladienes-ac in general[3] additional forces must be provided to stabilise the helical shape of components. Aggregation can best be explained by considering the hydrogen-bond pattern of dimeric pyrromethenones as known from X-ray studies.[24] If each of the two individuals is complemented to a bilirubin molecule the planar hypothetical dimer P_2 is formed (Fig. 5). Assemblies H_2^A and H_2^B which each are compounded from two helical conformers

* For toluene [Fig. 4(*c*)] this phenotype is only arrived at if spectra are extrapolated to infinite dilution. The end spectrum is not accessible experimentally owing to the large K_{dim}.

† The only thorough studies in this field described hitherto refer to tetrahydrofuran (THF)[15] and MTHF.[14] However, UV–VIS spectra for MTHF solutions as delineated in ref. 14 are partly incorrect in that no change in phenotype occurs at the lowest concentration.

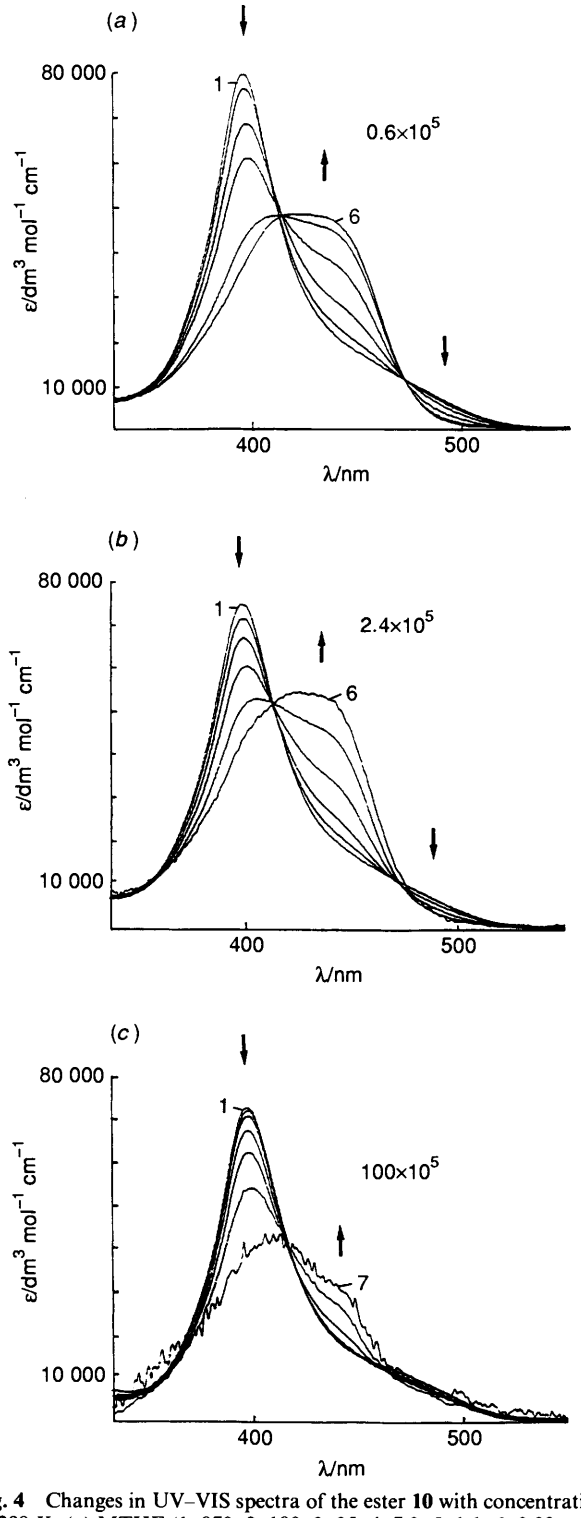

Fig. 4 Changes in UV–VIS spectra of the ester **10** with concentration at 298 K: (*a*) MTHF (1, 870; 2, 180; 3, 35; 4, 7.0; 5, 1.1; 6, 0.23 μmol dm^{-3}); (*b*) chloroform (1, 990; 2, 200; 3, 40; 4, 7.9; 5, 1.6; 6, 0.32 μmol dm^{-3}); (*c*) toluene (1, 870; 2, 170; 3, 35; 4, 7.0; 5, 1.1; 6, 0.23; 7, 0.079 μmol dm^{-3}). The numbers inserted refer to the corresponding dimerisation constant (K_{dim}/dm^3 mol^{-1}).

H can be formally derived from $\mathbf{P}_2$ by torsion of the non-hydrogen bonded pyrromethenone moieties around the axis dissecting the C-10 methylene spacers by about 150° in different and similar directions, respectively. Thereby in structure $\mathbf{H}_2{}^A$ the pyrromethenone–pyrromethenone hydrogen-bond pattern is repeated. On the other hand, rotation by about 80° affords two dimers $\mathbf{R}_2$ (only one shown) consisting of two ridge-tile like conformers **R**. For compound **10** only associates $\mathbf{H}_2{}^A$ and $\mathbf{H}_2{}^B$ fit the expectations derived from UV–VIS spectra. Even if modified these structures correlate with those tentatively suggested by Lightner *et al.*[12] but no decision between these alternatives could be made. Only $\mathbf{H}_2{}^A$ represents a closed structure in that all hydrogen bonding sites are occupied and should therefore resist further association. On the other hand in the dimer $\mathbf{H}_2{}^B$ two pyrromethenone halves are, at best, poorly hydrogen bonded and the formation of oligomers $\mathbf{H}_n{}^B$ can be expected to occur. An unequivocal assignment * of dimeric **10** to the assembly $\mathbf{H}_2{}^A$ can be accomplished by a comparison of its associative properties with those of the bridged analogues **4** and **6**, which—for geometric reasons—can only aggregate *via* dimer $\mathbf{H}_2{}^B$. Even at the lowest concentration accessible to vapour pressure osmometry (VPO) (*ca.* 1 mmol dm^{-3} solutions) the ester **10** in benzene, chloroform † and THF is present as a dimer (M_{obs} *ca.* 1225, n_{obs} 2, Fig. 2) which persists even if the concentration is raised by a factor of 20. The corresponding dimerisation constants (K_{dim}) as available from UV–VIS spectroscopy exhibit a pronounced susceptibility towards the hydrogen-bonding ability of the solvent (see inserts Fig. 4). The associative behaviour of the 2,18-bridged analogues **4** and **6** is quite different from that of **10**. In THF **4** is present as a monomer (n_{obs} 1, Fig. 2) and in chloroform association is low. In benzene, finally, the apparent mass M_{obs} of **4** and **6** steadily increases with concentration (Fig. 2) but no asymptotic convergence to n_{obs} 2 occurs and at the largest concentrations accessible, M_{obs} pronouncedly exceeds that of a dimer. If for the bilirubin **4** dimerisation constants K_{dim} are tentatively calculated for the four lower concentrations they increase from 420 to 55 700 mol^{-1} dm^3 (Table 3). Hence, the non-closed structure $\mathbf{H}_2{}^B$ comprises no stable species and gives rise to the formation of higher aggregates $\mathbf{H}_n{}^B$. Excellent fitting of experimental data in terms of an oligomerisation process can be accomplished for compound **4** by using equal microscopic association constants (*k ca.* 240 mol^{-1} dm^3).

The UV–VIS spectra of monomeric and predominantly (>70%) associated species of the bilirubin **4** are almost superimposable (Fig. 6) and provide further interesting detail in that intermolecular exciton coupling in aggregates $\mathbf{H}_2{}^B$ and $\mathbf{H}_n{}^B$ does not occur. The same can be expected for type $\mathbf{H}_2{}^A$ since the relative arrangements of pyrromethenone halves are pairwise the same.

The striking association tendency of the ester **10** (*cf.* inserts Fig. 4) has produced considerable confusion in the literature because UV–VIS spectra of biladienes-ac lacking acid or amide functional groups in poor hydrogen bonding solvents may differ considerably from each other even with respect to the phenotype but mostly refer to the dimer.‡ The exceedingly large K_{dim} values if compared with those of the bridged bilirubin **4** and pyrromethenones in general (K_{dim} *ca.* 1700 mol^{-1} dm^3, dichloromethane)[26] suggests that self-assembly of structure $\mathbf{H}_2{}^A$ *via* two sequential pairings of two pyrromethenone fragments takes place with positive cooperativity. The isosbestic points displayed by the UV–VIS spectra [Fig. 4(*a*) and 4(*b*)] are consistent with this hypothesis.

* Attempts to differentiate between these two assemblies by NOE difference spectra failed. Only the NOE enhancement between 10-H_2 of one constituent and the 2-Me of the second could be observed, however, which fits the expectations for both.

† By the same method M_{obs} 850 has been reported[15] for **10**.

‡ The spectra reported for **10** in dichloromethane,[16] MTHF,[14,16,25] carbon tetrachloride and chloroform[23] solutions (see also ref. 11, p. 385 and literature cited therein) are indicative of the predominance of the dimer rather than the monomer. The rough obeyance of Beer's law[5,14–16] comprises no adequate means to exclude association in poor hydrogen bonding solvents within a given and usually narrow concentration range. Analogously, if conformation persists on aggregation (Fig. 6) this criterion must necessarily fail.

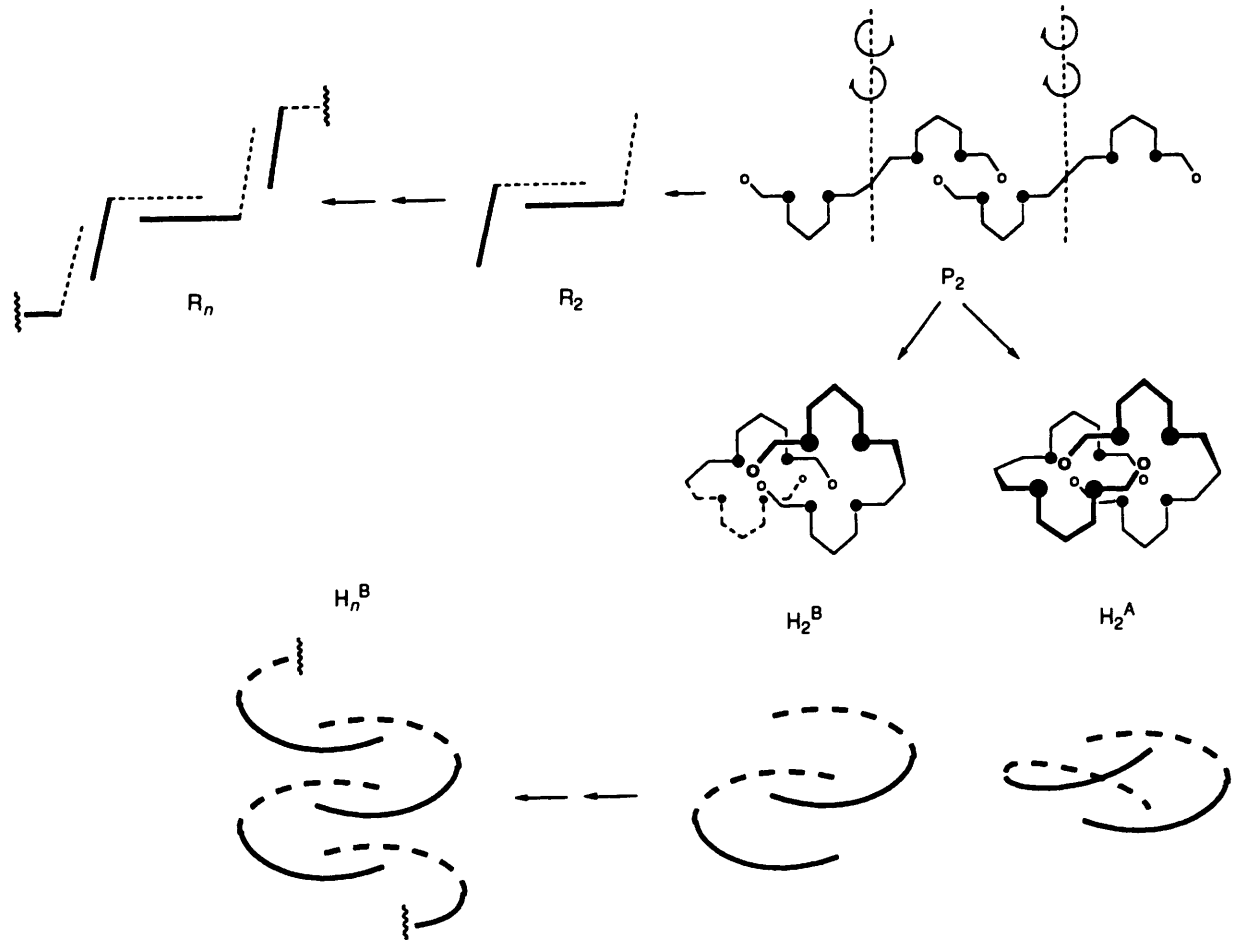

Fig. 5 Minimum representation of structures and topologies of biladiene-ac dimers $\mathbf{R}_2$, $\mathbf{H}_2^A$ and $\mathbf{H}_2^B$ and oligomers $\mathbf{R}_n$ and $\mathbf{H}_n^B$, and their genesis from the hypothetical planar assembly $\mathbf{P}_2$. Other potential assemblies made up from ridge-tile like conformers than those drawn for $\mathbf{R}_2$ and $\mathbf{R}_n$ have been omitted. For clarity structural drawings are restricted to the σ-backbones connecting the hydrogen bonding sites (●, N–H donor; ○, =O acceptor). For further details see text.

Table 3 Concentration *vs.* aggregation for the 2,18-bridged bilirubin **4** in benzene

c^a	$M_{obs}{}^b$	$K_{dim}{}^c$	$M_{calc}{}^d$
0.99	820	420	810
2.60	990	950	960
5.57	1 180	3 710	1 150
9.67	1 320	55 700	1 330
15.45	1 450	—	1 490

[a] c concentration applied (mmol dm^{-3}). [b] M_{obs} observed molecular mass (± 50) as determined by VPO at 310 K. [c] K_{dim} equilibrium constant calculated assuming dimerisation only (mol^{-1} dm^3). [d] $M_{calc} = \sum_i x_i n_i M_i$ calculated molecular mass through fitting to M_{obs} assuming oligomerisation (i = 1 . . . 5) with independent and equal microscopic equilibrium constants (k_i 240 mol^{-1} dm^3).

Due to the unsymmetrical substitution pattern of the ester **10** two diastereoisomeric forms of the dimer $\mathbf{H}_2^A$ are possible.* However since only 17-Vn increases the acceptor property of the lactam oxygen and as in general the formation of the strongest hydrogen bonds has priority,[27] preferential binding of like dipyrrinone halves seems most plausible. These expectations are in agreement with the homogeneity displayed by the low temperature ^{1}H NMR spectra (see below) and conform with considerations outlined in refs. 10 and 12.

* By analogy similar arguments apply to assemblies $\mathbf{H}_2^B$ and $\mathbf{H}_n^B$ relevant for the bridged compound **6**.

It also becomes evident that aggregated biladienes-ac of shape $\mathbf{H}_2^B$ and $\mathbf{H}_n^B$ can only become important if the geometry of the monomer is fixed *a priori*. Nevertheless, oligomeric species of **10** have been postulated[14] to occur at low temperatures in MTHF solution. However, constituents of these oligomers must be ridge-tile like as can be concluded from the phenotype of UV–VIS spectra in refs. 14, 16 and 25. Possibly, in MTHF a temperature controlled transition from the less polar structure $\mathbf{H}_2^A$ to the more polar associates of type $\mathbf{R}_2$ and $\mathbf{R}_n$ takes place. If this is true even the emission properties of **R** and $\mathbf{R}_n$ become indistinguishably similar to each other. This might explain hitherto seemingly contradictory results performed on **10** in MTHF by variable temperature absorption[14,16] and emission[16] spectroscopy.

Dynamic Properties.—The barriers to interconversion of the tetrapyrrole backbones of *M* and *P* chirality of the bridged compounds **2**–**6** were determined by kinetic measurements following the decay in optical activity of partially resolved materials with time. Partial resolution makes use of the strong heteroassociates formed between linear tetrapyrroles and (−)-(*R*)-cyclohexylhydroxyacetic acid and the concomitant discrimination between *M* and *P* helical species[17,28] resulting in a helical excess (h.e. 30–60%) of species with *M* chirality. By injecting the respective equilibrated mixtures into methanol or into methanolic sulfuric acid the influence of the chiral discriminator is withdrawn and reconstitution of the initial equilibria distinguished by h.e. = 0 takes place. This process was monitored by CD spectroscopy. The thermally induced

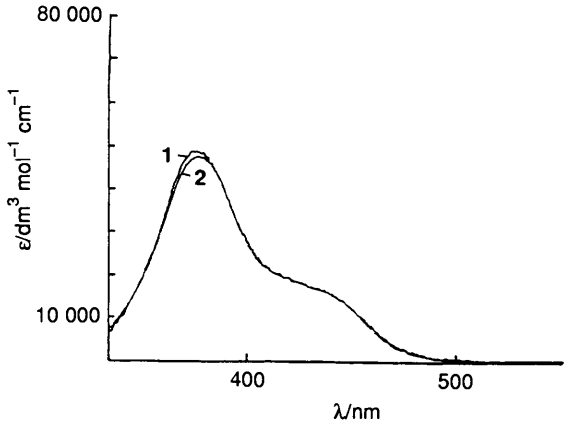

Fig. 6 UV–VIS spectra of the bilirubin **4** at 298 K for two different concentrations (1, 8.1; 2, 0.027 mmol dm^{-3}) in toluene

$M \rightleftharpoons P$ transitions proceed through continuous changes of torsional angles until rings A and D pass each other.* By an inspection of the graphic representation of the barrier heights (Fig. 7) it becomes apparent that the double bond in the bridge of compounds **5** and **6** increases kinetic stability by approximately the same amount (12–13 kJ mol^{-1}) if compared with **2** and **4**, respectively. This more generally reveals that differences in additional strain energy between biliverdins and bilirubins in the ground states by introduction of the bridge are only small which is prerequisite for a meaningful comparison of the bilirubin and biliverdin systems. The $\Delta G^{\ddagger}$-values of the protonated biliverdins **2**·H^+ and **5**·H^+ are found to be lower than those of the conjugated basic species but even larger than those of the corresponding bilirubins **4** and **6**. Clearly, if $M \rightleftharpoons P$ transitions in biliverdins take place, hydrogen bonds between nitrogens must be relaxed. Restrictions of that kind are absent in the bilirubins **3**, **4** and **6** and the protonated bilatrienes **2**·H^+ and **5**·H^+, too. Replacement of the double bond at C-10 for a single bond likewise contributes to the lowering of barriers. These results can be extended to non-bridged derivatives and suggest an increase in conformational mobility in the order bilatrienes-abc < protonated bilatrienes-abc < biladienes-ac. However, this holds true only if interferences with other hydrogen bonding groups or like molecules are absent. For example, the barrier of the 2,18-bridged ester **4** in methanol compared with that reported for bilirubin-IXα (**9**)[29] in chloroform: thereby restrictions are quite differently achieved owing to geometric constraints in **4** and to strong hydrogen bonding of the pyrromethenone moieties with the propionic acid side chains in **9**. Consequently using variable temperature ^{1}H NMR spectroscopy the barrier of compound **9** becomes unmeasurably low in methanol to which **4** refers. On the other hand on going from the ester **4** to the parent diacid **3** no characteristic changes occur (see Table 4).

If the difference in barriers between corresponding pairs of the restricted compounds **2** and **4** or **5** and **6** (*ca.* 9–11 kJ mol^{-1}) is subtracted from the value characteristic for open chain biliverdins (*ca.* 42–44 kJ mol^{-1})[30] the hypothetical barrier (*ca.* 31–35 kJ mol^{-1}) for a monomeric helical bilirubin is obtained. If part of a dimer, this barrier should be larger, increasing with decreasing polarity of the solvent. This prediction is nicely reflected in the $\Delta G^{\ddagger}$-values obtained for solutions of **10** in dichloromethane (*ca.* 40 kJ mol^{-1}, 180 K, see also ref. 16) and toluene (*ca.* 51 kJ mol^{-1}, 253 K). Under these conditions oligomers $\mathbf{R}_n$ are not formed as has been checked by UV–VIS spectroscopy.

* For the bilirubins **3**, **4** and **6** a second mechanism through cleavage of the C-9–C-10 or C-10–C-11 single bonds with subsequent recombination[11] can be excluded since acidic conditions were avoided and radical scavengers did not influence the rates of re-conversion.

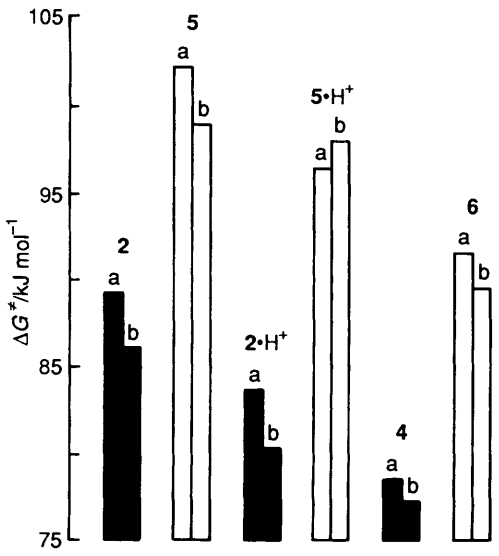

Fig. 7 Graphic representation of barriers to $M \rightleftharpoons P$ interconversion of the related triplets **2**/**2**·H^+/**4** (black bars) and **5**/**5**·H^+/**6** (blank bars) at 293 K. For further details see Table 4.

Table 4 Kinetic data for M ⇌ P interconversion of 2,18-bridged biliverdins and bilirubins[a]

		$t_{\frac{1}{2}}$[b]/s	K[c]	$k \times 10^3$[d]/s^{-1}	$\Delta G^{\ddagger}$[e]/kJ mol^{-1}
2[f]	**a**	207	4.0	0.70	89.4
	b			2.80	86.0
2·H^+[g]	**a**	19	4.0	7.34	83.7
	b			2.94	80.4
5	**a**	38 700	4.0	0.0036	102.3
	b			0.0143	98.9
5·H^+[g]	**a**	10 800	0.5	0.0428	96.2
	b			0.0214	97.9
3[h]	**a**	120	1.9	1.97	78.7
	b			3.81	77.3
4[h]	**a**	83	1.8	2.98	77.8
	b			5.37	76.5
6	**a**	673	2.3	0.311	91.5
	b			0.720	89.4

[a] By CD spectroscopy, *ca.* 3 × 10^{-5} mol dm^{-3} solutions in methanol; 293 K if not stated otherwise. [b] $t_{\frac{1}{2}}$ half life observed. [c] K equilibrium constant relating to equilibria (1) and (2) for the solvent applied as determined by ^{1}H NMR spectroscopy (see footnote *a* to Table 1). [d] k first-order rate constant of the individual species **a** and **b** obtained from $t_{\frac{1}{2}}$ and K. [e] $\Delta G^{\ddagger}$ barrier to interconversion (error ≤ |±0.2|). [f] The values are close to those reported for ethanol.[17] [g] In 0.25 mol dm^{-3} methanolic H_2SO_4. [h] At 266 K; the corresponding data in Fig. 7 (293 K) refer to extrapolated values by using $\Delta S^{\ddagger}$ *ca.* −30 J K^{-1} mol^{-1} estimated from the temperature dependence of barrier heights between 273 and 253 K.

Conclusions

The study presented allows for the first comprehensive view of the conformational pattern of biliverdins and bilirubins. The crucial factor responsible for their different conformational and associative behaviour is the hydrogen bonding site located at N-23 serving as acceptor and donor, respectively. In (4*Z*,10*Z*,-15*Z*) biliverdins hydrogen bonding between the pyrrolenine nitrogen and the hydrogens at the pyrrole and the two pyrrolinone rings determine the helical (5 *syn*,9 *syn*,14 *syn*) conformation. A destabilisation, if at all, can only be achieved by favourably oriented substituents[31,32] efficiently competing

with this intramolecular hydrogen bonding network. Regarding the (4*Z*,15*Z*) biladiene-ac backbone the acceptor sites are confined to the two lactam oxygens as long as appropriate substituent groups are absent. This holds true for the ester **10** and peralkylated bilirubins, too. In these cases hydrogen bonding can only occur intermolecularly through pyrromethenone–pyrromethenone pairing. If, in addition, interactions with the solvent are small self-assembly into closed dimeric aggregates $\mathbf{H_2}^A$ takes place in which constituents adopt helicoidal conformations of like helicities. The related but energetically less favourable type $\mathbf{H_2}^B$ becomes important only if the helicoidal conformation is preformed. Unlike dimer $\mathbf{H_2}^A$, $\mathbf{H_2}^B$ is prone to oligomerisation. On the other hand unrestricted biladienes-ac may, if at all, only oligomerise *via* the non-closed species $\mathbf{R}_2$ and $\mathbf{R}_n$. If competitors for the biladiene–biladiene hydrogen bonding are provided by the solvent or by an appropriate solute, aggregates $\mathbf{H_2}^A$ cannot be formed and the sterically favoured ridge-tile like geometry predominates. Suitable side chains, preferentially at C-8 and C-12, favour this arrangement,[3,33,34] simultaneously preventing homoassociation. A stabilisation of a helical like backbone geometry by undecanoic acid side chains has recently been reported.[35]

The more general relevance of our conformational considerations is provided by protonated bilatrienes.[36,37] On protonation the N-acceptor is lost and similar phenomena and conformational changes as observed for biladienes-ac arise.

Compounds **5** and **6** exhibit the largest barrier heights ever reported for biliverdins and bilirubins and are best suited for optical resolution.

Experimental

M.p.s were determined with a Kofler-Reichert hot-stage apparatus. ^{1}H NMR (250 or 400 MHz) and ^{13}C NMR (62.9 or 100.6 MHz; *J*-modulated) spectra were recorded with Bruker instruments (AC 250 AF, AM 400 WB) at 297 K for *ca.* 10^{-2} mol dm^{-3} solutions in $CDCl_3$ (chromatographed on alumina prior to use) [$^2H_5$]pyridine, [$^2H_4$]methanol, [$^2H_4$]methanol–[$^2H_2$]-sulfuric acid (0.25 mol dm^{-3}), [$^2H_6$]ethanol, [$^2H_6$]DMSO and [$^2H_6$]benzene using $SiMe_4$ as a reference. Variable temperature ^{1}H NMR spectra were performed in [$^2H_8$]toluene, [$^2H_5$]pyridine and CD_2Cl_2. *J*-Values are given in Hz. NOE difference spectra were obtained for 5×10^{-3} mol dm^{-3} deaerated solutions. Molecular masses have been determined by fast atom bombardment (FABMS, 3-nitrophenylmethanol or glycerol, Xe) and field desorption (FDMS) mass spectrometry using a Finnigan MAT 900 and a Finnigan MAT 8230 instrument, respectively. UV–VIS spectra were measured with a Perkin-Elmer Lambda 7 spectrometer (0.001–10 cm quartz cuvettes). Kinetic measurements were performed with a circular dichrograph (I.S.A. Jobin-Yvon, CD6) carrying thermostatted (±0.2 K) quartz cuvettes (1 cm). All optical measurements except those performed with the 0.001, 0.01 and 10 cm cuvettes were carried out in thermostatted cell compartments (± 1 K) for solutions in chloroform, benzene and toluene (Uvasol, Merck, all chromatographed on alumina prior to use), THF (p.A., Loba) and MTHF (zur Synthese, Fluka, both distilled twice over $LiAlH_4$ prior to use). Dichloromethane, methanol (Uvasol, Merck), pyridine (p.A., Riedel-de-Haën) and sulfuric acid (95–97%, p.A., Merck) were used as purchased. VPO measurements (M_{obs} ± 50) for solutions in THF (at 45 °C), chloroform and benzene (both at 37 °C) were obtained with a vapour pressure osmometer (Knauer, model 1990). The reference mass (610.7) was provided by biliverdin-IXα-dimethyl ester (**8**) which is known to be monomeric even at large concentrations.[15,18] The grade of solvents was the same as used for UV–VIS spectroscopy. Column chromatography was performed on silica gel (Kieselgel 60, 230–400 mesh, Merck) using methanol (p.A., Riedel-de-Haën), chloroform and acetone (both p.A., Loba, purified with silica gel prior to use) as eluents. For TLC Kieselgel 60 plates (Merck) were used. The optically active (−)-(*R*)-cyclohexylhydroxyacetic acid (Fluka) {$[\alpha]_D^{20}$ −22.5° (*c* 1, acetic acid)} used showed satisfactory optical rotation. For syntheses methanol (p.A., Riedel-de-Haën), sulfuric acid (95–97%, p.A., Merck) and sodium borohydride (zur Synthese, Merck) were used. After column chromatography the compounds were triturated with benzene (**3**, **5a** and **5b**) or hexane (**4** and **6**) (0.1–0.5 cm^3). After addition of pentane (3–8 cm^3) and sonication (5 min) the respective mixture was centrifuged and the supernatant discarded. The microcrystalline powder was then dried under reduced pressure.

General Remarks on the Handling of the Bilirubins.—The sensitivity of the bridged bilirubins **3**, **4** and **6** towards oxygen (re-oxidation to the corresponding verdins) and light ($Z \rightarrow E$ isomerisations) by far exceeds that known for open chain analogues like **9** and **10**. Moreover, even in the crystalline state at −18 °C slow decomposition occurs. Therefore all solvents used in syntheses, purification, VPO measurements and spectral recordings were deaerated by at least two freeze-pump-thaw cycles using argon as protecting gas and all manipulations were carried out in dim yellow light under argon. All measurements reported here refer to freshly prepared solutions of freshly prepared compounds. Though less critical the same precautions were taken for compound **10**.

[(P, 1′R) + (M, 1′S)]- *and* [(M, 1′R) + (P, 1′S)]-(4*Z*,9*Z*,-15*Z*,3′*Z*)-2,18-(1′-*Methoxybut*-3′-*en*-1′,4′-*diyl*)-8,12,-*bis*(2″-*methoxycarbonylethyl*)-3,7,13,17-*tetramethyl*-1,19-*dioxo*-1,19,-21,24-*tetrahydrobilin* (**5a** *and* **5b**).—A slurry of the biliverdin **2**[8] (120 mg, 0.18 mmol) in sulfuric acid (10 cm^3) was sonicated for 1 min at 0 °C and then poured into cooled (−20 °C) methanol (150 cm^3). **CAUTION**! After 3 min the dark green solution was treated with aqueous $NaHCO_3$ (10%, *ca.* 330 cm^3) and subsequently stripped with chloroform (2 × 200 cm^3). The combined blue extracts were washed with brine (2 × 50 cm^3), dried (Na_2SO_4) and the solvent evaporated under reduced pressure. At this stage the proportion **5a**/**5b** can be controlled within a certain range by equilibration of the residue (40 °C, 3 h) in the appropriate solvent (Table 1) prior to chromatography. Evaporation of the solvent and column chromatography [2 × 18 cm, chloroform–acetone (7% v/v)] afforded **5b** and **5a** in that order (total 60 mg, 52%), the proportions being consistent with those in Table 1.

Compound **5a** had m.p. 115–119 °C [Found: C, 67.1; H, 6.2; N, 8.3. $C_{36}H_{40}N_4O_7$ (640.7) requires C, 67.5; H, 6.3; N, 8.7%]; *m/z* (FDMS) 640 (M^+); for UV–VIS, ^{1}H NMR and ^{13}C NMR spectra see Tables 2, 5 and 6 and Fig. 1.

Compound **5b** had m.p. 115–119 °C [Found: C, 66.7; H, 6.1; N, 8.2. $C_{36}H_{40}N_4O_7$ (640.7) requires C, 67.5; H, 6.3; N, 8.7%]; *m/z* (FDMS) 640 (M^+); for UV–VIS, ^{1}H NMR and ^{13}C NMR spectra see Tables 2, 5 and 6 and Fig. 1.

If the above reaction was performed with deuteriated reagents using [$^2H_4$]methanol and [$^2H_2$]sulfuric acid deuterium was only found in the 1′-OMe groups of **5a** and **5b** as revealed by ^{1}H NMR spectroscopy.

Sodium Borohydride Reductions of the Bridged Biliverdins **1**, **2** *and* **5**.—*General procedure.* A stirred solution of the bridged biliverdin (0.08 mmol, 51–54 mg) in methanol (15 cm^3) was treated with small portions (5 × 10 mg, 1.3 mmol) of sodium borohydride in intervals of 1 min at 4 °C. During this period the colour had changed from blue to light yellow and the reaction was immediately quenched with water (150 cm^3) containing acetic acid (0.08 cm^3, 1.4 mmol). After extraction with chloroform (3 × 70 cm^3) the organic layer was washed

Table 5 ^{1}H NMR spectra of bridged tetrapyrroles and their assignment[a]

2a[b]	11.84 (1 H, s, 22, 23-H), 9.52 (2 H, s, 21-, 24-H), 7.46 (1 H, s, 10-H), 6.61 (2 H, s, 5-, 15-H), 4.29 (2 H, d, *J* 10, 1'-, 4'-H), 3.64 (6 H, s, CO_2Me), 3.27 (6 H, s, 1'-, 4'-OMe), 3.12 (4 H, m, 8-, 12-CH_2), 2.70 (4 H, m, CH_2–CO_2), 2.7–2.0 (4 H, m, 2'-, 3'-H_2), 2.39 and 2.19 (6 H × 2, s, 3-, 7-, 13-, 17-Me)
2b[b]	12.90 (1 H, s, 22, 23-H), 10.17 (2 H, s, 21-, 24-H), 7.29 (1 H, s, 10-H), 6.48 (2 H, s, 5-, 15-H), 4.90 (2 H, br s, 1'-, 4'-H), 3.64 (6 H, s, CO_2Me), 3.32 (6 H, s, 1'-, 4'-OMe), 3.05 (4 H, m, 8-, 12-CH_2), 2.71 (4 H, m, CH_2–CO_2), 2.7–2.0 (4 H, m, 2'-, 3'-H_2), 2.58 (6 H, s, 3-, 17-Me), 2.13 (6 H, s, 7-, 13-Me)
4a	10.57 and 10.53 (2 H × 2, s, 21-, 22-, 23-, 24-H), 6.37 (2 H, s, 5-, 15-H), 4.11 (2 H, d, *J* 11, 1'-, 4'-H), 4.04 (2 H, s, 10-H_2), 3.6–2.0 (4 H, m, 2'-, 3'-H_2), 3.60 (6 H, s, CO_2Me), 3.15 (6 H, s, 1'-, 4'-OMe), 3.2–2.0 (8 H, m, 8-, 12-CH_2–CH_2–CO_2), 2.27 (6 H, s, 3-, 17-Me), 2.04 (6 H, s, 7-, 13-Me)
4b	10.58 and 10.23 (2 H × 2, s, 21-, 22-, 23-, 24-H), 6.39 (2 H, s, 5-, 15-H), 4.81 (2 H, br s, 1'-, 4'-H), 3.97 (2 H, s, 10-H_2), 3.6–2.0 (4 H, m, 2'-, 3'-H_2), 3.61 (6 H, s, CO_2Me), 3.23 (6 H, s, 1'-, 4'-OMe), 3.2–2.0 (8 H, m, 8-, 12-CH_2–CH_2–CO_2), 2.52 (6 H, s, 3-, 17-Me), 2.07 (6 H, s, 7-, 13-Me)
5a	12.07 (1 H, s, 22-, 23-H), 9.52 and 8.97 (1 H × 2, s, 21-, 24-H), 7.45 (1 H, s, 10-H), 6.75 (2 H, s, 5-, 15-H), 6.40 (1 H, d, *J* 11, 4'-H), 6.13 (1 H, dt, *J* 11, *J* 11, *J* 7, 3'-H), 4.42 (1 H, dd, *J* 10.5, *J* 1, 1'-H), 3.83 and 2.83 (1 H × 2, m, 2'-H_2), 3.62 and 3.60 (3 H × 2, s, CO_2Me), 3.26 (3 H, s, 1'-OMe), 3.09 (4 H, m, 8-, 12-CH_2), 2.70 (4 H, m, CH_2–CO_2), 2.40 (3 H, s, 3-Me), 2.38 (3 H, s, 17-Me), 2.20 (6 H, s, 7-, 13-Me)
5b[c]	11.85 (1 H, br s, 22-, 23-H), 9.38 and 9.17 (1 H × 2, br s, 21-, 24-H), 7.48 (1 H, s, 10-H), 6.68 (1 H, s, 5-H), 6.65 (1 H, s, 15-H), 6.58 (1 H, d, *J* 12, 4'-H), 6.31 (1 H, m, 3'-H), 4.55 (1 H, d, *J* 5.5, 1'-H), *ca.* 3.4 and *ca.* 2.7 (1 H × 2, m, 2'-H_2), 3.62 and 3.60 (3 H × 2, s, CO_2Me), 3.38 (3 H, s, 1'-OMe), 3.09 (4 H, m, 8-, 12-CH_2), 2.70 (4 H, m, CH_2–CO_2), 2.57 (3 H, s, 3-Me), 2.33 (3 H, s, 17-Me), 2.20 (3 H, s, 13-Me), 2.19 (3 H, s, 7-Me)
6a[d]	10.77, 10.62, 10.28 and 10.00 (1 H × 4, s, 21-, 22-, 23-, 23-H), 6.39 (1 H, s, 5-H), 6.38 (1 H, s, 15-H), 6.37 (1 H, d, *J* 11, 4'-H), 5.97 (1 H, dt, *J* 11, *J* 11, *J* 7.5, 3'-H), 4.18 (1 H, d, *J* 10, 1'-H), 4.02 and 3.88 (2 H, AB, *J* 19, 10-H_2), *ca.* 3.8 and 2.66 (1 H × 2, m, 2'-H_2), 3.65 and 3.61 (3 H × 2, s, CO_2Me), 3.16 (3 H, s, 1'-OMe), 2.5–2.1 (8 H, m, 8-, 12-CH_2–CH_2–CO_2), 2.32 (3 H, s, 3-Me), 2.28 (3 H, s, 17-Me), 2.12 (3 H, s, 7-Me), 2.08 (3 H, s, 13-Me)
6b[d]	10.77, 10.55, 10.28 and 9.76 (1 H × 4, s, 21-, 22-, 23-, 24-H), 6.52 (1 H, d, *J* 12, 4'-H), 6.40 (1 H, s, 5-H), 6.32 (1 H, s, 15-H), 6.11 (1 H, ddd, *J* 12, *J* 9, *J* 8, 3'-H), 4.77 (1 H, t, *J* 3.5, 1'-H), 4.03 and 3.80 (2 H, AB, *J* 19, 10-H_2), 3.66 and 3.60 (3 H × 2, s, CO_2Me), 3.29 (3 H, s, 1'-OMe), *ca.* 2.9 (2 H, m, 2'-H_2), 2.5–2.1 (8 H, m, 8-, 12-CH_2–CH_2–CO_2), 2.58 (3 H, s, 3-Me), 2.18 (3 H, s, 17-Me), 2.15 (3 H, s, 7-Me), 2.11 (3 H, s, 13-Me)

[a] Chemical shifts (δ) downfield from $SiMe_4$ for *ca.* 10^{-2} mol dm^{-3} solutions in [$^2H_5$]pyridine, 297 K, at 250 MHz; assignments by NOE and homonuclear decoupling experiments; for the ^{1}H NMR spectra of **3** and **10** see Experimental. [b] For spectra in $CDCl_3$ benzene and methanol see refs. 8 and 36. [c] Some of the signals are exceptionally broad at ambient temperatures especially those due to the N–H protons. These effects are also observed in benzene and chloroform, and are less pronounced at 313 K. On lowering the temperature down to 236 K two distinct sets of N–H signals appear (ratio 1:1, coalescence of 22,23-H at 280 K, $\Delta\nu$ 460 Hz, corresponding to $\Delta G^{\ddagger}$ *ca.* 52 kJ mol^{-1}) which suggests a conformational inhomogeneity originating from the C_4 bridge. [d] At 400 MHz.

Table 6 ^{13}C NMR spectra of bridged tetrapyrroles and their assignment[a]

	4[b]		**5**[c]		**6**	
	a	**b**	**a**	**b**	**a**	**b**
CO_2Me	175.43–	175.43–	173.10–	173.10–	173.40– and	173.37–
1-CO, 19-CO	172.47– and	173.68–	168.44–, 167.13–	168.20–, 168.32–	172.64– and 172.51– and	172.19–
=CH-3'			132.16+	131.88+	130.20+	128.74+
=CH-4'			124.80+	122.69+	124.34+	122.97+
=CH-10			114.26+	114.07+		
=CH-5, =CH-15	102.50+	101.91+	98.76+, 98.44+	98.37+, 98.21+	99.0+–98.9+	
CH-1'	76.99+	79.68+	74.59+	79.80+	75.29+	79.27+
1'-(4'-)OMe	56.29+	57.17+	55.91+	56.93+	55.74+	56.86+
CO_2Me	52.12+	52.12+	51.50+	51.50+	51.37+ and	51.34+
CH_2CO_2	35.87–	35.87–	35.78–	35.78–	35.41–, 35.27– and	35.15–
CH_2-2'-(-3')	28.85–	27.12–	33.61–	30.01–	32.93–	32.70–
CH_2-10	23.91–	23.84–			23.12–	23.12–
8-CH_2, 12-CH_2	20.77–	20.82–	20.31–	20.31–	19.79–, 19.45–	20.00–, 19.74–
3-Me, 17-Me	10.03+ and	9.69+	11.37+, 9.91+	10.96+, 10.53+	11.76+, 9.64+	11.88+, 10.15+
7-Me, 13-Me	9.45+	9.45+	9.42+, 9.34+	9.42+, 9.34+	9.46+, 9.38+	9.52+, 9.35+

[a] Chemical shifts (δ) downfield from $SiMe_4$ for *ca.* 10^{-2} mol dm^{-3} solutions in [$^2H_5$]pyridine; signs refer to *J*-modulated ^{13}C NMR spectra; 100.6 MHz; 303 K; carbons not listed have not been assigned. [b] In [$^2H_4$]methanol. [c] At 62.9 MHz.

successively with aqueous $NaHCO_3$ (50 cm^3) and water (50 cm^3) and then dried (Na_2SO_4). After evaporation of the solvent under reduced pressure, purification and eventual separation into diastereoisomers **a** and **b** was performed as described for the individual compounds (yields 90–95%).

[(P, 1'R,4'R) + (M, 1'S,4'S)]- *and* [(M, 1'R,4'R) + (P, 1'S,4'S)]-(4Z,15Z)-2,18-(1',4'-*Dimethoxybutan*-1',4'-*diyl*)-8,12-*bis*(2''-*hydroxycarbonylethyl*)-3,7,13,17-*tetramethyl*-1,19-*dioxo*-1,10,19,21,23,24-*hexahydrobilin* (**3a** *and* **3b**). These compounds were prepared from the verdin **1**[32] according to the general procedure. The crude material was chromatographed on a short column (1 × 5 cm, chloroform–methanol 12% v/v) to give an inseparable, rapidly interconverting mixture of the acids **3a** and **3b**; no m.p., gradually decomposing on heating up to 230 °C [Found: C, 63.8; H, 6.4; N, 8.2. $C_{35}H_{42}N_4O_8$ (646.7) requires C, 65.0; H, 6.5; N, 8.7%]; *m/z* (negative FABMS) 645 (M^- – H); δ_H(400 MHz, $CDCl_3$, 297 K): major isomer **3a** (64%): 8.82 (2 H, br s, CO_2H), 6.08 (2 H, s, 5-, 15-H), 3.88 (2 H, d, *J* 11, 1'-, 4'-H), 4.02 (2 H, s, 10-H_2), 3.15 (6 H, s, 1'-, 4'-OMe), 3.0–1.6 (4 H, m, 2'-, 3'-H_2), 2.7–2.5 (4 H, m, 8-, 12-CH_2), *ca.* 2.3 (4 H, m, CH_2CO_2) and 2.08 (6 H × 2, s, 3-, 7-, 13-, 17-Me); minor isomer **3b** (36%): 8.66 (2 H, br s, CO_2H), 6.06 (2 H, s, 5-, 15-H), 4.40

(2 H, br s, 1'-, 4'-H), 3.98 (2 H, s, 10-H_2), 3.24 (6 H, s, 1'-, 4'-OMe), 3.0–1.6 (4 H, m, 2'-, 3'-H_2), 2.7–2.5 (4 H, m, 8-, 12-CH_2), *ca.* 2.3 (4 H, m, CH_2CO_2), 2.19 and 2.08 (6 H × 2, s, 3-, 7-, 13-, 17-Me); for UV–VIS spectra see Table 2.

Dimethyl esters of **3a** *and* **3b**, **4a** *and* **4b**. These compounds were prepared from **2**[8] following the general procedure. The crude material was chromatographed on a short column [1 × 5 cm, chloroform–methanol (3% v/v)] to give an inseparable, rapidly interconverting mixture of the esters **4a** and **4b**; m.p. 120–125 °C [Found: C, 64.6; H, 6.7; N, 8.1. $C_{37}H_{46}N_4O_8$ (674.8) requires C, 65.9; H, 6.9; N, 8.3%]; *m/z* (positive FABMS) 674 (M^+); for UV–VIS, ^{1}H NMR and ^{13}C NMR spectra see Tables 2, 5 and 6 and Figs. 3 and 6.

[(P, 1'R) + (M, 1'S)]- *and* [(M, 1'R) + (P, 1'S)]-(4Z,15Z,-3'Z)-2,18-(1'-*Methoxybut*-3'-*en*-1',4'-diyl)-8,12-*bis*(2''-*methoxycarbonylethyl*)-3,7,13,17-*tetramethyl*-1,19-*dioxo*-1,10,19,21,23,-24-*hexahydrobilin* (**6a** *and* **6b**). These compounds were prepared from the verdin **5** according to the general procedure. The crude material was subjected to preparative TLC at −10 °C using a mixture of toluene–ethyl acetate–propan-2-ol–pyridine 70:19:10:1 as the mobile phase (R_f**6b** > R_f**6a**). Extractions of the individual zones with methanol–pyridine (0.5% v/v) and evaporation of the solvent under reduced pressure (< 0.01 Torr) was performed at −15 °C. With exception of the UV–VIS spectra of **a** and **b** species in methanol (Table 2) all other properties were determined at room temperature and therefore refer to the isomeric mixtures (Table 1); compound **6** had m.p. 135–140 °C [Found: C, 66.7; H, 6.5; N, 8.4. $C_{36}H_{42}N_4O_7$ (642.7) requires C, 67.3; H, 6.6; N, 8.7%]; *m/z* (positive FABMS) 642 (M^+); for UV–VIS, ^{1}H NMR and ^{13}C NMR spectra see Tables 2, 5 and 6.

Bilirubin-IXα-*dimethyl Ester* (**10**).—This compound was prepared according to ref. 38. ^{1}H NMR spectra in $CDCl_3$ and CD_2Cl_2 are in agreement with those reported in the literature.[10,16] NOE enhancements (2–10%) in $CDCl_3$ conform with the (4*Z*,15*Z*,5 *syn*,14 *syn*) geometry in agreement with ref. 10. In addition intermolecular NOE enhancements 10-H_2 ↔ 2-Me (*ca.* 1%) were observed. δ_H([$^2H_8$]toluene, 250 MHz, 297 K): 11.62 (1 H, s, 21-H), 10.87 (1 H, s, 22-H), 10.60 (1 H, s, 23-H), 10.47 (1 H, s, 24-H), 6.24, 5.14 and 5.12 (1 H × 3, XBA, J_{XB} 17.5, J_{XA} 11.5, J_{BA} 1, 3-Vn), 6.21 (1 H, s, 5-H), 6.05, 5.47 and 4.83 (1 H × 3, XMA, J_{XM} 18, J_{XA} 11.5, J_{MA} 2, 18-Vn), 5.84 (1 H, s, 15-H), 4.37 (2 H, s, 10-H_2), 3.45 and 3.44 (3 H × 2, s, CO_2Me), 3.06 (4 H, m, 8-, 12-CH_2), 2.53 (4 H, m, CH_2CO_2), 1.97 (6 H, s, 7-, 13-Me) and 1.59 (6 H, s, 2-, 17-Me); δ_H([$^2H_8$]toluene, 250 MHz, 223 K): 12.07 (1 H, s, 21-H), 11.10 (1 H, s, 22-H), 10.73 (1 H, s, 24-H), 10.64 (1 H, s, 23-H), 6.25 (1 H, s, 5-H), 6.15 (1 H, dd, *J* 18, *J* 11, 3-Vn-H_X), 6.01, 5.50 and 4.77 (1 H × 3, XMA, J_{XM} 18, J_{XA} 11.5, J_{MA} 2, 18-Vn), 5.81 (1 H, s, 15-H), 5.06 (2 H, m, 3-Vn-H_{AB}), 4.58 and 4.29 (1 H × 2, AB, J_{AB} 15, 10-H_2), 3.42 and 3.40 (3 H × 2, s, CO_2Me), 3.20 and 3.03 (2 H × 2, m, 8-, 12-CH_2), 2.53 (4 H, m, CH_2CO_2), 1.92 and 1.84 (3 H × 2, s, 7-, 13-Me), 1.52 and 1.46 (3 H × 2, s, 2-, 17-Me); coalescence of 10-H_2 at 253 K.

Partial Resolutions and Kinetic Measurements.—Bilirubins **3**, **4** *and* **6**. A stock solution of the corresponding compound in toluene (*ca.* 3 × 10^{-4} mol dm^{-3}) containing 10 equivalents of (−)-(*R*)-cyclohexylhydroxyacetic acid was equilibrated (CD control). An aliquot (0.2 cm^3) of the respective solution was then injected into cuvettes containing pre-thermostatted methanol (2 cm^3). Initial CD-values [$\Delta\varepsilon$/dm^3 mol^{-1} cm^{-1} (λ/nm)] at t = 0 for two selected monitor wave lengths: **3** (266 K) −51 (455), +55 (392); **4** (266 K) −49 (450), +61 (392); **6** (293 K) −61 (444), +78 (386) (h.e. *ca.* 35%).*

Biliverdins **2**, **2**·H^+, **5** *and* **5**·H^+. Stock solutions of **2** and **5**, respectively, in toluene (*ca.* 10^{-2} mol dm^{-3}) containing 3 equivalents of (−)-(*R*)-cyclohexylhydroxyacetic acid were equilibrated (CD control). An aliquot of the respective solution (0.01 cm^3) was then injected into pre-thermostatted cuvettes containing 2 cm^3 of variable mixtures of methanol and sulfuric acid equivalent to the following portions of unprotonated and protonated species (in parenthesis): 0.0 mol dm^{-3} (100:0), 0.0007 mol dm^{-3} (90:10), 0.007 mol dm^{-3} (50:50), 0.07 mol dm^{-3} (10:90), and 0.25 mol dm^{-3} (< 5: > 95). The large amount of sulfuric acid necessary to ensure complete protonation is owing to the conformation dependent basicity of biliverdins[36,39] being exceptionally low for helically fixed members. Initial CD-values [$\Delta\varepsilon$/dm^3 mol^{-1} cm^{-1} (λ/nm)] at t = 0 for two selected monitor wave lengths (293 K): **2** −50 (650), +71 (385) (h.e. *ca.* 35%);[17] **2**·H^+ −48 (720), +77 (382) (h.e. *ca.* 35%); **5** −66 (646), +128 (376) (h.e. *ca.* 60%); **5**·H^+ −63 (728), +145 (386) (h.e. *ca.* 60%).*

The decrease in optical activity was followed by CD spectroscopy at different wavelengths. First-order rate constants k_{obs} were calculated from ln ΔA *vs.* time plots and were linear for at least 3 half lives. From this quantity and the equilibrium distribution K of **a** and **b** species in methanol and methanol–sulfuric acid, respectively, the individual parameters were calculated (Table 4 and Fig. 7). Rates were independent from the monitor wave length chosen. Likewise, neither did the addition of a radical scavenger (2,6-di-*tert*-butyl-4-methylphenol) nor the presence of a base (pyridine, 1% v/v; unprotonated compounds only) influence the rates. For **2**·H^+ the influence of sulfuric acid beyond protonation can be neglected. This follows from the linear dependence of k_{obs} from the mole fractions of protonated species present in the respective solution as determined by UV–VIS spectrometry. Owing to the acidity dependent equilibrium constant K (Table 4) this does not apply to **5**·H^+.

* Complete resolution and chiroptical properties of compounds **5** and **6** will be the subject of a future report.[28] Owing to the low barriers to helix interconversions of compounds **3** and **4** the corresponding h.e.s achieved could not be determined.

Acknowledgements

This work has been supported by the *Hochschuljubiläumsstiftung der Stadt Wien* and by the *Fonds zur Förderung der wissenschaftlichen Forschung in Österreich* (Nos. P3574, P5767, P6537C and P8202C). Mass spectra were kindly provided by Dr. G. Remberg (Göttingen, Germany) and by Application Laboratory Finnigan MAT (Dr. M. Holin, Bremen, Germany). NMR spectra taken with the AM 400 WB instrument were kindly provided by Dr. H. Kählig (this institute).

References

1 R. Huber, *Angew. Chem.*, 1989, **101**, 849; *Angew. Chem. Int. Ed. Engl.*, 1989, **28**, 848; H. Scheer, *Angew. Chem.*, 1981, **93**, 230; *Angew. Chem. Int. Ed. Engl.*, 1981, **20**, 241; T. W. Goodwin, *Chemistry and Biochemistry of Plant Pigments*, Academic Press, New York, 1976, 2nd edn., vol. 1, p. 328; A. Bennett and H. W. Siegelman, *Bile Pigments of Plants*, in *The Porphyrins*, ed. D. Dolphin, Academic Press, New York, 1979, vol. 6, pp. 493–520; W. Rüdiger and F. Thümmler, *Angew. Chem.*, 1991, **103**, 1242; *Angew. Chem. Int. Ed. Engl.*, 1991, **30**, 1216; H. Mohr, *Endeavour*, 1977, **1**, 107; K. Schaffner, S. E. Braslavsky and A. R. Holzwarth, *Adv. Photochem.*, 1990, **15**, 229.

2 D. A. Lightner and A. F. McDonagh, *Acc. Chem. Res.*, 1984, **17**, 417; R. B. Frydman and B. Frydman, *Acc. Chem. Res.*, 1987, **20**, 250.

3 H. Falk, *The Chemistry of Linear Oligopyrroles and Bile Pigments*, Springer-Verlag, Wien–New York, 1989.

4 M. Choussy and M. Barbier, *Helv. Chim. Acta*, 1975, **58**, 2651; M. Bois-Choussy and M. Barbier, *Heterocycles*, 1978, **9**, 677; J. B. Iturraspe, S. Bari and B. Frydman, *J. Am. Chem. Soc.*, 1989, **111**, 1525.

5 W. Kufer, H. Scheer and A. R. Holzwarth, *Isr. J. Chem.*, 1983, **23**, 233.
6 R. B. Frydman, S. Bari, M. L. Tomaro and B. Frydman, *Biochem. Biophys. Res. Commun.*, 1990, **171**, 465.
7 P. Nesvadba and A. Gossauer, *J. Am. Chem. Soc.*, 1987, **109**, 6545.
8 D. Krois and H. Lehner, *J. Chem. Soc., Perkin Trans. 1*, 1989, 2179; D. Krois and H. Lehner, *Monatsh. Chem.*, 1989, **120**, 575.
9 H. Falk and K. Thirring, *Tetrahedron*, 1981, **37**, 761.
10 D. Kaplan and G. Navon, *J. Chem. Soc., Perkin Trans. 2*, 1981, 1374; D. Kaplan and G. Navon, *Isr. J. Chem.*, 1983, **23**, 177.
11 A. F. McDonagh, *Bile Pigments: Bilatrienes and 5,15-Biladienes*, in *The Porphyrins*, ed. D. Dolphin, Academic Press, New York, 1979, vol. 6, pp. 293–491.
12 F. R. Trull, J.-S. Ma, G. L. Landen and D. A. Lightner, *Isr. J. Chem.*, 1983, **23**, 211.
13 P. Manitto, G. S. Ricca and D. Monti, *Gazz. Chim. Ital.*, 1974, **104**, 633.
14 H. Falk and N. Müller, *Monatsh. Chem.*, 1982, **113**, 111.
15 H. Falk, T. Schlederer and P. Wolschann, *Monatsh. Chem.*, 1981, **112**, 199.
16 A. R. Holzwarth, E. Langer, H. Lehner and K. Schaffner, *Photochem. Photobiol.*, 1980, **32**, 17.
17 D. Krois and H. Lehner, *Monatsh. Chem.*, 1989, **120**, 789; D. Krois and H. Lehner, *J. Chem. Soc., Perkin Trans. 2*, 1989, 2085.
18 H. Lehner, S. E. Braslavsky and K. Schaffner, *Liebigs Ann. Chem.*, 1978, 1990.
19 R. Bonnett and A. F. McDonagh, *J. Chem. Soc., Perkin Trans. 1*, 1973, 881; H. Falk, K. Grubmayr, E. Haslinger, T. Schlederer and K. Thirring, *Monatsh. Chem.*, 1978, **109**, 1451.
20 G. Blauer and G. Wagnière, *J. Am. Chem. Soc.*, 1975, **97**, 1949; G. Blauer, *Isr. J. Chem.*, 1983, **23**, 201.
21 D. A. Lightner, J. K. Gawroński and W. M. D. Wijekoon, *J. Am. Chem. Soc.*, 1987, **109**, 6354.
22 R. Bonnett, J. E. Davies, M. B. Hursthouse and G. M. Sheldrick, *Proc. R. Soc. London*, Ser. B, 1978, **202**, 249; G. LeBas, A. Allegret, Y. Mauguen, C. DeRango and M. Bailly, *Acta Crystallogr., Sect. B*, 1980, **36**, 3007.
23 D. A. Lightner, T. A. Wooldridge and A. F. McDonagh, *Biochem. Biophys. Res. Commun.*, 1979, **86**, 235.
24 D. L. Cullen, P. S. Black, E. F. Meyer Jr., D. A. Lightner, G. B. Quistad and C. S. Pak, *Tetrahedron*, 1977, **33**, 477; D. L. Cullen, G. Pepe, E. F. Meyer Jr., H. Falk and K. Grubmayr, *J. Chem. Soc., Perkin Trans. 2*, 1979, 999.
25 A. R. Holzwarth and K. Schaffner, *Photochem. Photobiol.*, 1981, **33**, 635.
26 H. Falk, K. Grubmayr, G. Höllbacher, O. Hofer, A. Leodolter, F. Neufingerl and J. Ribó, *Monatsh. Chem.*, 1977, **108**, 1113.
27 M. C. Etter, *Acc. Chem. Res.*, 1990, **23**, 120.
28 D. Krois and H. Lehner, manuscript submitted.
29 P. Manitto and D. Monti, *J. Chem. Soc., Chem. Commun.*, 1976, 122.
30 H. Lehner, W. Riemer and K. Schaffner, *Liebigs Ann. Chem.*, 1979, 1798.
31 D. Krois and H. Lehner, *J. Chem. Soc., Perkin Trans. 2*, 1990, 1745; D. Krois and H. Lehner, *Monatsh. Chem.*, 1991, **122**, 89.
32 H. Falk, N. Müller and H. Wöss, *Monatsh. Chem.*, 1987, **118**, 1301.
33 D. A. Lightner, T. C. Adams and J. S. Ma, *Tetrahedron*, 1984, **40**, 4253.
34 D. A. Lightner, M. Reisinger and G. L. Landen, *J. Biol. Chem.*, 1986, **261**, 6034.
35 J. Chiefari, R. V. Person and D. A. Lightner, *Tetrahedron*, 1992, **48**, 5969.
36 D. Krois, *Monatsh. Chem.*, 1991, **122**, 495.
37 E. Haidl, D. Krois and H. Lehner, *Monatsh. Chem.*, 1985, **116**, 119.
38 W. Küster, Hoppe-Seyler's *Z. Physiol. Chem.*, 1924, **141**, 40.
39 S. Bari, R. B. Frydman, C. Grosman and B. Frydman, *Biochem. Biophys. Res. Commun.*, 1992, **188**, 48.

Paper 3/00554B
Received 28*th January* 1993
Accepted 15*th March* 1993